

# Stochastic Electron Acceleration in Shell-Type Supernova Remnants

Siming Liu<sup>1</sup>, Zhong-Hui Fan<sup>2,3</sup>, Christopher L. Fryer<sup>1,4</sup>, Jian-Min Wang<sup>2,5</sup>, and Hui Li<sup>1</sup>

## ABSTRACT

We study the stochastic electron acceleration by fast mode waves in the turbulent downstream of weakly magnetized collisionless astrophysical shocks. The acceleration is most efficient in a dissipative layer, and the model characteristics are determined by the shock speed, density, magnetic field, and turbulence decay length. The model explains observations of shell-type supernova remnants RX J1713.7-3946 and J0852.0-4622 and can be tested by observations in hard X-rays with the *HXMT* and *NuSTAR* or  $\gamma$ -rays with the *GLAST*.

*Subject headings:* acceleration of particles — MHD — plasmas — shock waves — turbulence

## 1. Introduction

Recent observations of high-energy emission from a few shell-type supernova remnants (STSNRs) advance our understanding of the underlying physical processes significantly (Enomoto et al. 2002). These observations not only give high quality emission morphology and spectra (Uchiyama et al. 2003; Aharonian et al. 2004; Cassam-Chenaï et al. 2004; Hiraga et al. 2005; Takahashi et al. 2008a), which lead to tight upper limits on thermal X-rays, but also discover X-ray variability on a timescale of a few months (Uchiyama et al. 2007), which is intimately connected to processes near the shock front (SF). The radio to X-ray emissions are produced by relativistic electrons through the synchrotron processes. The nature of the TeV emission is still a matter of debate. The major challenges to the

---

<sup>1</sup>Los Alamos National Laboratory, Los Alamos, NM 87545; liusm@lanl.gov

<sup>2</sup>Institute of High Energy Physics, Chinese Academy of Sciences, Beijing 100049, China

<sup>3</sup>Department of Physics, Yunnan University, Kunming 650091, Yunnan, China

<sup>4</sup>Physics Department, The University of Arizona, Tucson, AZ 85721

<sup>5</sup>Theoretical Physics Center for Science Facilities, Chinese Academy of Sciences

hadronic scenario include: 1) the lack of correlation between the TeV emission and molecular cloud distribution; 2) the requirement of very high mean target gas density, supernova explosion energy, and/or proton acceleration efficiency, which implies efficient magnetic field amplification in the context of the diffusive shock acceleration and strong suppression of the electron acceleration (Lucek & Bell 2000; Berezhko & Völk 2006; Butt et al. 2008); 3) the good correlation between the X-ray and TeV emission (Plaga 2008; Aharonian et al. 2006, 2007a), which suggests a leptonic scenario. Because secondary leptons from hadronic processes won't produce as much radiation power as  $\gamma$ -rays from neutral pion ( $\pi^0$ ) decays (Aharonian et al. 2007b), the fact that the X-ray luminosity is slightly higher than the TeV luminosity requires that most leptons be accelerated from the background plasma.

Compared to the hadronic scenario, the leptonic scenario has much fewer parameters and is well-constrained by the observed radio, X-ray, and TeV spectra. In the simplest one-zone model, the TeV emission is produced through the inverse Compton (IC) scattering of the Galactic interstellar radiation by the same relativistic electrons producing the radio and X-rays (Porter et al. 2006). The TeV spectrum can be used to infer the high-energy electron distribution. One then needs to fit both the synchrotron spectral shape and flux level by adjusting the magnetic field alone. TeV observations always see spectral softening with the increase of the photon energy, suggesting a spectral cutoff (Aharonian et al. 2007a,b). There are also indications that the synchrotron spectrum cuts off in the hard X-ray band (Takahashi et al. 2008a,b; Uchiyama et al. 2007). A single power-law model with an exponential cutoff for the electron distribution has difficulties in reproducing the broad TeV spectrum. Models with more gradual cutoffs lead to much better fits. Relativistic particle distributions with gradual high-energy cutoffs are a natural consequence of the stochastic acceleration (SA) by plasma waves in magnetized turbulence (Park & Petrosian 1995; Becker, Le & Dermer 2006; Stawarz & Petrosian 2008). The particle distribution is determined by the interplay among the acceleration, cooling, and escape processes with the cutoff shape determined by the energy dependence of the ratio of the acceleration to cooling or escape rate. Given the low magnetic fields derived from leptonic models, the radiative cooling time is much longer than the remnant lifetime. The gradual high-energy cutoff has to be caused by the balance between the acceleration and escape processes.

We consider the evolution of weakly magnetized turbulence in the downstream of strong non-relativistic shocks and study the SA by fast mode waves. The large scale turbulence cascades following the Kolmogorov phenomenology (Boldyrev 2002; Jiang et al. 2008) until it reaches the scale, where the eddy turnover time becomes comparable to the period of fast mode waves. The Iroshnikov-Kraichnan phenomenology prevails on even smaller scales. The collisionless damping of plasma waves sets in at the coherent length of the magnetic field, where the eddy turnover time is comparable to the period of Alfvén waves. Fast mode

waves propagating nearly parallel to the mean magnetic field can survive the transit-time damping (TTD) by the thermal background particles, and accelerate some electrons through cyclotron resonances to a power-law high-energy distribution, which cuts off at the energy, where the particle gyro-radius reaches the coherent length of the magnetic field (Liu et al. 2006). Acceleration of higher energy electrons by the nearly isotropic fast mode waves on larger scales leads to a gradual cutoff. SA of electrons can naturally account for emissions from the STSNRs with a weak magnetic field. Future observations in the hard X-ray and MeV bands may test the model. The particle acceleration model is described in § 2 and applied to SNRs RX J1713-3946 and J0852.0-4622 to derive quantitative results in § 3. § 4 gives the conclusions.

## 2. Turbulence Cascade, Wave Damping, and Stochastic Particle Acceleration

The collisionless nature of weakly magnetized shocks implies difficulties in converting the free energy in the system into heat and energetic particles instantaneously at a narrow SF. Instead, the high magnetic Reynolds number implies strong turbulence. Previous studies of diffusive shocks focus on its roles in making high-energy particles crossing the SF repeatedly. The turbulence can also carry a significant fraction of the released free energy and decay gradually. The turbulence generation mechanism is not well understood. It is usually attributed to the Weibel instability (Weibel 1959) of particle streaming and may also depend on the properties of the upstream plasma. We here assume that the turbulence is isotropic and generated at a scale  $L$  with an eddy speed  $u$ . The free energy dissipation rate is then given by  $Q = C_1 \rho u^3 / L$ , where  $C_1 \sim 1$  is dimensionless. For strong non-relativistic shocks with the shock frame upstream speed  $U$  much higher than the speed of the upstream fast mode waves  $v_F = (v_A^2 + 5v_S^2/3)^{1/2}$ , mass, momentum, and energy conservations across the SF require  $U^2 = 5v_S^2 + 5u^2 + 2v_A^2 + U^2/16$ , where the Alfvén speed  $v_A = (B^2/4\pi\rho)^{1/2}$ , the isothermal sound speed  $v_S = (P/\rho)^{1/2}$ , and  $B$ ,  $\rho$ ,  $P$  are the magnetic field, mass density, pressure, respectively. The shock structure can be complicated due to the presence of strong turbulence, and the speeds  $v_S$ ,  $v_A$ , and  $u$  should be considered as averaged quantities over  $\sim L$ , which also corresponds to the energy dissipation scale. The excitation of plasma waves should be very efficient in the supersonic phase with  $u \geq v_F$ , and the waves may prevail in the downstream accelerating some particles in the background plasma to very high energies.

The eddy turnover speed and time are given respectively by  $v_{edd}^2(k) = 4\pi W(k)k^3$  and  $\tau_{edd}(k) = 2\pi/C_1 k v_{edd}$ , where  $W(k) = (4\pi)^{-1}(2\pi Q/C_1\rho)^{2/3}k^{-11/3}$ ,  $k = 2\pi/l$ , and  $l$  are the isotropic turbulence power spectrum, wave number, and eddy size, respectively. At the turbulence generation scale  $k_m = 2\pi/L$ ,  $v_{edd} = u$ , and the total turbulence energy is given

by  $\int W(k)4\pi k^2 dk = (3/2)u^2$ . The MHD wave period is given by  $\tau_F(k) = 2\pi/v_F k$ . Then the transition scale from the Kolmogorov to Kraichnan phenomenology  $k_t$  occurs at  $\tau_F(k_t) = \tau_{edd}(k_t)$ , which gives  $k_t = (C_1 u/v_F)^3 k_m$ . For  $k > k_t$ , the turbulence spectrum in the inertial range is given by

$$W(k) = (4\pi)^{-1} (v_F/C_1)^{1/2} u^{3/2} k_m^{1/2} k^{-7/2}. \quad (1)$$

The collisionless damping starts at the coherent length of the magnetic field  $l_d = 2\pi/k_d$ , where the period of Alfvén waves  $2\pi/kv_A$  is comparable to the eddy turnover time,  $k_d = (C_1^3 u^3 v_F/v_A^4) k_m$ .

Both  $v_A$  and  $v_S$  may be lower than  $u$  near the SF. If  $u \gg v_A \gg v_S$  at the SF, fast, slow, and Alfvén waves can all be excited, and the consequent plasma heating quickly leads to  $v_S \geq v_A$ . Fast mode waves with the highest phase speed should dominate the SA processes. We assume that they dominate the energy dissipation as the turbulent flow moves away from the SF and  $v_F$  evolves from  $v_A$  to  $u$  at the same time. For a fully ionized hydrogen plasma with isotropic particle distributions, which are reasonable in the absence of strong large scale magnetic fields, the TTD rate is given by (Stix 1962; Quataert 1998; Petrosian et al. 2006)

$$\Lambda_T(\theta, k) = \frac{(2\pi k_B)^{1/2} k \sin^2 \theta}{2(m_e + m_p) \cos \theta} \left[ (T_e m_e)^{1/2} \exp\left(-\frac{m_e \omega^2}{2k_B T_e k_{\parallel}^2}\right) + (T_p m_p)^{1/2} \exp\left(-\frac{m_p \omega^2}{2k_B T_p k_{\parallel}^2}\right) \right], \quad (2)$$

where  $T_e, T_p, m_e, m_p, \theta, \omega$ , and  $k_{\parallel} = k \cos \theta$  are the electron and proton temperatures, masses, angle between the wave propagation direction and mean magnetic field, wave frequency, and parallel component of the wave vector, respectively. The first and second terms in the brackets on the right hand side correspond to damping by electrons and protons, respectively. For weakly magnetized plasma with  $v_A < v_S$ , proton heating always dominates the TTD for  $\omega^2/k_{\parallel}^2 \sim v_S^2 \sim 2k_B T_p/m_p$  (Quataert 1998). If  $v_A$  does not change dramatically in the downstream, the continuous heating of background particles through the TTD processes makes  $T_p \rightarrow (m_p/m_e)T_e$  since the heating rates are proportional to  $(mT)^{1/2}$ , where  $m$  and  $T$  represent the mass and temperature of the particles, respectively. Parallel propagating waves with  $\sin \theta = 0$  are not subject to the TTD. Obliquely propagating waves are damped efficiently by the background particles. Although the damping rates for waves propagating nearly perpendicular to the magnetic field with  $\cos \theta \simeq 0$  are also low, these waves are subject to damping by magnetic field wandering (Petrosian et al. 2006). The turbulence power spectrum cuts off sharply when the damping rate becomes comparable to the turbulence cascade rate  $\Gamma = \tau_{edd}^{-2}/(\tau_F^{-1} + \tau_{edd}^{-1}) \simeq \tau_{edd}^{-2} \tau_F$  (Jiang et al. 2008). One can define a critical propagation angle  $\theta_c(k)$ , where  $\Lambda_T(\theta_c, k) = \Gamma(k)$ . Then for  $k_B T_p = C_{2p} m_p u^2$  with  $C_{2p} < 3/5$

for  $v_F < u$ , equations (1) and (2) give

$$\frac{v_A^2 k_d^{1/2}}{2^{1/2} \pi^{3/2} C_{2p}^{1/2} u v_F k^{1/2}} \simeq \frac{\sin^2 \theta_c}{\cos \theta_c} \exp\left(-\frac{v_F^2}{2C_{2p} u^2 \cos^2 \theta_c}\right).$$

where the electron pressure and damping have been ignored.

For  $v_A \ll U$ , we have  $3v_F^2/5 \simeq v_S^2 \simeq C_{2p} u^2 = [3C_{2p}/16(C_{2p} + 1)]U^2$ . The acceleration and scattering times of relativistic electrons by these nearly parallel propagating waves are energy independent and given, respectively, by  $\tau_{sc} = 2\pi/ck_d$ , and  $\tau_{ac} = (3c^2/v_F^2)\tau_{sc}$  (Liu et al. 2006; Blandford & Eichler 1987), where  $c$  is the speed of light. The electron escape time from the large scale eddies is given by  $\tau_{esc} = L^2/4c^2\tau_{sc}$ , and the spectral index of the accelerated electrons in the steady state is given by  $p = (9/4 + \tau_{ac}/\tau_{esc})^{1/2} - 1/2 = (9/4 + 12c^2 v_A^8 / C_1^6 u^6 v_F^4)^{1/2} - 1/2$ . The maximum energy that electrons can reach is given by  $\gamma_c m_e c^2 = 2\pi q B / k_d = 7.26[(p + 0.5)^2 - 2.25]^{1/2} [C_{2p}/(C_{2p} + 1)]^{1/2} (L/10^{18} \text{cm})(B/10 \mu\text{G})U_0$  TeV, where  $U_0 = U/0.015c$ ,  $q$  is the elementary charge units. The ratio of the dissipated energy carried by non-thermal particles to that of the thermal particles should be greater than  $\eta = \theta_c^2(k_d)/2 = e^{5/6} v_A^2 / 2\pi(2\pi C_{2p})^{1/2} u v_F$ , where  $e = 2.72$ , since the isotropic turbulence with  $k < k_d$  can also accelerate particles with the Lorentz factor  $\gamma \geq \gamma_c$ .

Electrons with even higher energy interact with the nearly isotropic fast mode waves at  $k < k_d$ . The corresponding acceleration and escape times are proportional to  $\gamma^{1/2}$  and  $\gamma^{-1/2}$ , respectively, which leads to a steady-state electron distribution  $f \propto \exp -(\gamma/\gamma_c)^{1/2}$  for  $\gamma \gg \gamma_c$  (Park & Petrosian 1995; Becker, Le & Dermer 2006). To obtain the complete electron distribution from the thermal energy to the high-energy cutoff self-consistently, one needs to obtain the acceleration and scattering rates by these nearly parallel propagating (with  $k > k_d$ ) and nearly isotropic (with  $k < k_d$ ) fast mode waves and solve the particle kinetic equation numerically. These are beyond the scope of this paper. Instead, the above discussions indicate that the particle distribution may be approximated reasonably well by  $f \propto \gamma^{-p} \exp -(\gamma/\gamma_c)^\beta$  with  $\beta = 1/2$ . To have significant particle acceleration, the acceleration time needs to be shorter than the turbulence decay time:  $\tau_{ac} < \tau_{edd}(k_m) = L/C_1 u$ , which also validates the usage of the steady-state solution of the particle kinetic equation and implies  $C_1 < (20C_{2p})^{1/2}/3[(p + 0.5)^2 - 2.25]^{1/2}$ .

### 3. Results

Several STSNRs have been observed extensively in the radio, X-ray, and TeV bands. X-ray observations with *Chandra*, *XMM-Newton*, and *Suzaku*, and TeV observations with HESS have made several surprising discoveries that challenge the classical diffusive shock particle

acceleration model. The SNR RX J1713.7-3946 is about  $t = 1600$  years old (Wang et al. 1997) with a radius of  $R \simeq 10$  pc and a distance of  $D \simeq 1$  kpc. By fitting its broad-band spectrum with the above electron distribution and background photon field given by Porter et al. (2006) through the synchrotron and IC processes, we find that  $p = 1.85$ ,  $B = 12.0 \mu\text{G}$ ,  $\gamma_c m_e c^2 = 3.68$  TeV, and the total energy of electrons with  $\gamma > 1800$  (Liu et al. 2006; Fan et al. 2008),  $E_e = 3.92 \times 10^{47}$  erg (Fig. 1). The thin line shows the best fit with  $\beta = 1$ , whose TeV spectrum is not broad enough to explain the HESS observations. In the hard X-ray band, our model predicted emission spectrum is significantly harder and brighter, which gives better fit to the *Suzaku* observations and can be tested with future *HXMT* and *NuSTAR* observations. Our model also predicts a higher MeV flux testable with future *GLAST* observations. Figure 2 shows the dependence of the spectrum on  $p$  and  $\beta$ .

The distribution of relativistic electrons obtained above implies  $L = 2.34 \times 10^{17} [C_{2p}/(C_{2p} + 1)]^{-1/2} U_0^{-1}$  cm, and the electron density  $n_e = 2.00 \times 10^{-3} (C_{2p} + 1)^{5/4} C_1^{-3/2} C_{2p}^{-1/2} U_0^{-5/2}$  cm $^{-3}$ , where  $Y \simeq 0.1$  is the Helium abundance. For the steady-state solution to be applicable,  $C_1 < 0.824 C_{2p}^{1/2} < 0.64$ . For  $C_{2p} = C_1 = 0.5$ , we have  $L = 4.04 \times 10^{17} U_0^{-1}$  cm,  $n_e = 1.33 \times 10^{-2} U_0^{-5/2}$  cm $^{-3}$ ,  $\tau_{ac} = 138 U_0^{-2}$  yrs,  $\tau_{esc} = 42.3 U_0^{-2}$  yrs, and  $\eta = 0.384\% U_0^{1/2}$ . The energy carried by the magnetic field  $E_B = B^2 R^2 L / 2 = 2.77 \times 10^{46} U_0^{-1}$  erg. The short coherent length of the magnetic field  $2\pi/k_d = \gamma_c m_e c^2 / qB = 1.02 \times 10^{15}$  cm is consistent with the low level of polarization from most part of the radio image (Lazendic et al. 2004). If  $k_d$  doesn't change significantly in the downstream, the distance that relativistic electrons diffuse through the  $t = 1600$  yr lifetime of the remnant is about  $(t/\tau_{esc})^{1/2} L = 0.805$  pc. Most of them are therefore trapped near the SF. The total kinetic energy carried by the supersonic dissipative layer in the lab frame is  $K \simeq 2\pi R^2 L (1 + 2Y) m_p n_e (3U/4)^2 = 7.34 \times 10^{48} U_0^{-3/2}$  erg. The corresponding gas mass  $M = 2K/(3U/4)^2 = 1.29 \times 10^{32} U_0^{-7/2}$  g, thermal energy  $E_t \simeq 6\pi R^2 L m_p n_e (1 + 2Y) v_S^2 = 3.67 \times 10^{48} U_0^{-3/2}$  erg, gas temperature  $k_B T_p = 2m_p (1 + 2Y) E_t / 3M (1 - Y) = 26.4 U_0^2$  keV, where we have assumed that the temperatures of protons and Helium ions are the same and  $T_e \ll T_p$ .

The acceleration efficiency of  $\sim \eta$  is not sensitive to  $p$  and  $U$  and therefore doesn't change significantly through the evolution of the SNR, implying that a thermal energy of  $E_e/\eta \sim 1.02 \times 10^{50} U_0^{-1/2}$  erg, which is 27.8 times higher than  $E_t$ , be produced in accompany with the electron acceleration. The mass of the shocked thermal plasma is about  $E_e M / \eta E_t \simeq 3.58 \times 10^{33} U_0^{-5/2}$  g =  $1.79 U_0^{-5/2} M_\odot$ . These suggest that most of the relativistic electrons were accelerated more than  $\tau_{ac} \sim 100$  years before outside the current dissipative layer. If the shocked plasma is uniformly distributed within a shell of 4.5 pc (Aharonian et al. 2006), the electron density is  $1.74 \times 10^{-2} U_0^{-5/2}$  cm $^{-3}$ , which is comparable to that inferred from X-ray observations (Cassam-Chenaï et al. 2004).

However, X-ray observations of the north-west outer edge of the remnant suggests  $U < 0.015c$  (Uchiyama et al. 2007). So the model predicted thermal X-ray emission likely exceeds the observed value. The north-west edge is interacting with dense molecular clouds. It is possible that the shock speed in a low density medium is still greater than the observed upper limit so that  $U \geq 0.015c$ . On the other hand, given the uncertainties in the collisionless electron heating processes, the electron temperature may be well below 1.0 keV so that no significant thermal X-ray emission is expected in the *XMM-Newton* and *Chandra* X-ray bands. Coulomb collisions will make  $k_B T_e \simeq 0.198(n_e/0.01\text{cm}^{-3})^{2/5}(t/1600\text{yr})^{2/5}U_0^{4/5}$  keV (Hughes et al. 2000). Line emission dominates the cooling with a luminosity of  $\sim 10^{33}$  erg  $\text{s}^{-1}$  and may be observed in the UV to soft X-ray band. Detailed modeling of the evolution of the SNR is needed to reach more quantitative results (Decourchelle et al. 2000).

X-ray observations discover thin bright features varying on a timescale of about a year. The width of these features is about  $w \sim 4''0 \simeq 6.0 \times 10^{16}$  cm, corresponding to a speed  $\geq 0.063c$ . Since the shock speed is much less than this value, the variability has been attributed to cooling in very strong magnetic fields (Uchiyama et al. 2007). According to our model, the decay may be due to the diffusive escape of relativistic electrons from bright regions. For electrons with a scattering mean free path of  $2\pi/k_d$ , the corresponding diffusive escape time from a region of size  $w$  is about 0.93 years. The X-rays are produced by electrons with energies greater than  $\gamma_c m_e c^2$ , whose scattering mean free path by fast mode waves should be longer than  $2\pi/k_d$  implying a diffusion timescale of a few months. The formation of these bright features is then related to the inhomogeneity in the pre-shock medium, which is supported by the relatively higher level of radio polarization nearby (Lazendic et al. 2004). The fact that the brightening features are not located at the outer edge of the remnant can be attributed to the projection effect.

We also apply the model to SNR RX J0852.0-4622. For  $d = 1$  kpc,  $R = 17$  pc, we have  $B = 9.4 \mu\text{G}$ ,  $p = 2$ ,  $\gamma_c m_e c^2 = 2.94$  TeV ( $\gamma_c = 5.76 \times 10^6$ ), and the electron energy  $E_e = 1.01 \times 10^{48}$  erg. These imply  $L = 3.73 \times 10^{17}U_0^{-1}$  cm,  $n_e = 7.76 \times 10^{-3}U_0^{-5/2}$   $\text{cm}^{-3}$ ,  $\tau_{ac} = 141U_0^{-2}$  years,  $\tau_{esc} = 35.3U_0^{-2}$  years,  $\eta = 0.404\%U_0^{1/2}$ ,  $K = 1.14 \times 10^{49}U_0^{-3/2}$  erg,  $M \simeq 2.01 \times 10^{32}U_0^{-7/2}$  g,  $E_t = 5.71 \times 10^{48}U_0^{-3/2}$  erg,  $k_B T_p = 26.4U_0^2$  keV, and  $E_B = B^2 R^2 L/2 = 4.53 \times 10^{46}U_0^{-1}$  erg. These two remnants are very similar.

#### 4. Conclusions

The steady-state distribution of relativistic electrons accelerated by fast mode waves in a downstream turbulent dissipative layer with a thickness  $L$  of weakly magnetized collisionless

astrophysical shocks can be approximated as

$$f \propto \gamma^{-p} \exp -(\gamma/\gamma_e)^{1/2},$$

where  $p = (9/4 + 2^{25}3^3c^2v_A^8/5^2U^{10})^{1/2} - 1/2$ ,  $\gamma_e m_e c^2 = qBL5^{1/2}[(p + 0.5) - 2.25]^{1/2}U/24c$  for  $C_1 = C_{2p} = 0.5$ , and the ratio of the dissipated energies going into nonthermal and thermal particles is  $\sim \eta = (e^{5/3}96/5\pi^3)^{1/2}v_A^2/U^2$ . For  $p > 2.09$ , the turbulence decay time is shorter than the particle acceleration time and one needs to consider the time dependent solution. The accelerated electrons in the STSNRs give excellent fits to the broadband spectra of SNRs RX J1713.7-3946 and J0852.0-4622. The model attributes the recently observed variable X-ray features to inhomogeneity in the upstream and the spatial diffusion of relativistic electrons near the cutoff energy and predicts harder hard X-ray spectrum, higher hard X-ray and  $\gamma$ -ray fluxes than leptonic models with a sharper cutoff in the electron distribution. Future high sensitivity hard X-ray and  $\gamma$ -ray observations will test the model. The major uncertainty of the model is related to the turbulence generation mechanism near the collisionless SF. In this paper, we assume that the turbulence is isotropic and has a characteristic eddy size of  $L$ . Little is known about the evolution of anisotropic turbulence. The latter is valid as far as the free energy dissipation through shocks proceeds over the scale  $L$ , instead of, instantaneously at a narrow region ( $\ll L$ ) near the SF as suggested in the diffusive shock models.

This work was supported in part under the auspices of the US Department of Energy by its contract W-7405-ENG-36 to Los Alamos National Laboratory and by the NSF of China (grants 10325313, 10733010, 10521001, and 10778726), CAS key project (grant KJCX2-YW-T03), the Postdoctoral Foundation of China (grant 20070410636). We thank Dr. Lu, F. J. for discussions on the instrument sensitivities.

## REFERENCES

- Aharonian, F. A., et al. 2004, *Nature*, 432, 75
- Aharonian, F. A., et al. 2006, *A&A*, 449, 223
- Aharonian, F. A., et al. 2007a, *A&A*, 464, 235
- Aharonian, F. A., et al. 2007b, *ApJ*, 661, 236
- Becker, P. A., Le, T., Demer, C. D. 2006, *ApJ*, 647, 539B
- Berezhko, E. G., & Völk, H. J. 2006, *A&A*, 451, 981

- Blandford, R., & Eichler, D. 1987, PhR, 154, 1
- Boldyrev, S. 2002, ApJ, 569, 841
- Butt, Y. M., Porter, T. A., Katz, V., & Waxman, E. 2008, MNRAS, 386, L20
- Cassam-Chenaï, G., et al. 2004, A&A, 427, 199
- Decourchelle, A., Ellison, D. C., & Ballet, J. 2000, ApJ, 329, L29
- McEnery, J. E., Moskalenko, I. V., & Jonathan, F. O. 2004, ASSL, 304, 361
- Enomoto, R., et al. 2002, Nature, 416, 823
- Fan, Z. H., Liu, S. M., Wang, J. M., Fryer, C. L., & Li, H. 2008, ApJ, 673, L139
- Hughes, J. P., Rakowski, C. E., & Decourchelle, A. 2000, ApJ, 543, L61
- Hiraga1, J. S., Uchiyama, Y., Takahashi, T., & Aharonian, F. A. 2005, A&A 431, 953
- Jiang, Y. W., Liu, S. M., Petrosian, V., Fryer, C. L., & Li, H. 2008, astro-ph/0802.0910
- Lazendic, J. S., et al. 2004, ApJ, 602, 271
- Li, T. P., Zhang, S. N., & Lu, F. J. 2006, <http://scholar.lib.cn/A-kjkxxb2006z1007.html>
- Liu, S. M., Melia, F., Petrosian, V., & Fatuzzo, M. 2006, ApJ, 647, 1099
- Lucek, S. G., & Bell, A. R. 2000, MNRAS, 314, 65
- Park, B. T., & Petrosian, V. 1995, ApJ, 446, 699
- Petrosian, V., & Liu, S. 2004, ApJ, 610, 550
- Petrosian, V., Yan, H. R., & Lazarian, A. 2006, ApJ, 644, 603
- Plaga, R. 2008, NewA, 13, 73
- Porter, T. A., Moskalenko, I. V., & Strong, A. W. 2006, ApJ, 648L, 29
- Quataert, E. 1998, ApJ, 500, 978
- Stawarz, L., & Petrosian, V. 2008, astro-ph/0803.0989
- Stix, T. H. 1962, The Theory of Plasma Waves (McGraw-Hill Book Company, inc.)
- Takahashi, T., et al. 2008a, PASJ, 60, 131

Takahashi, T., et al. 2008b, astro-ph/0806.1490

Uchiyama, Y., Aharonian, F. A., & Takahashi, T. 2003, A&A, 400, 567

Uchiyama, Y., et al. 2007, Nature, 449, 576

Wang, Z. R., Qu, Q.-Y., & Chen, Y. 1997, A&A, 318L, 59

Weibel, E. S. 1959, PRL, 2, 83

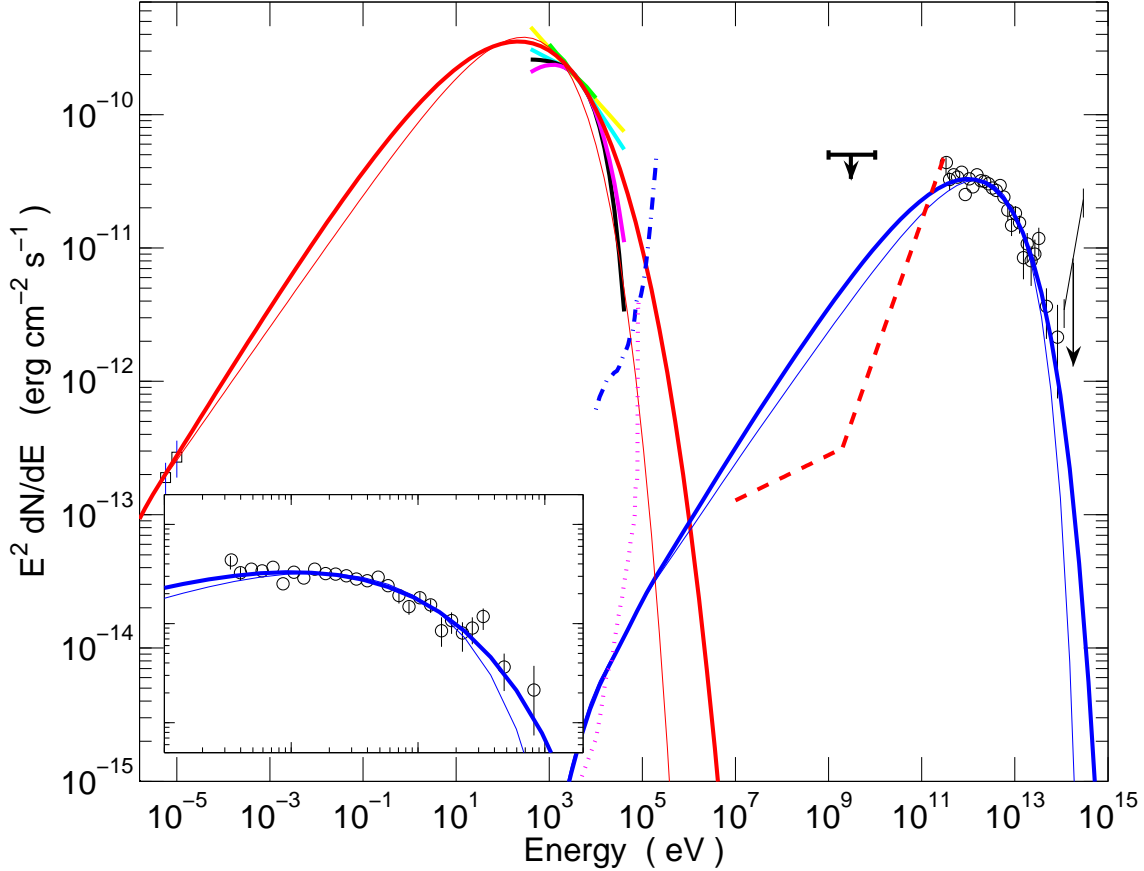


Fig. 1.— Model fit to the broadband spectrum of SNR RX J1713-3946. The low and high energy spectral humps are produced through the synchrotron and IC scattering of the Galactic interstellar radiation, respectively. The X-ray data are for the four models discussed in Takahashi et al. (2008a) and rescaled to the *ASCA* flux level for the whole remnant (Uchiyama et al. 2003). The thick solid line corresponds to the fiducial model with  $\beta = 0.5$ ,  $p = 1.85$ ,  $\gamma_c = 7.2 \times 10^6$ , and  $B = 12.0 \mu\text{G}$ . The thin solid line with  $p = 2.0$ ,  $B = 12.0 \mu\text{G}$ , and  $\gamma_c = 4.4 \times 10^7$  is the best for an electron distribution with an exponential cutoff, i.e.,  $\beta = 1.0$ . The fiducial model gives a better fit to the X-ray and TeV spectra. Insert is an enlargement of the TeV spectrum to demonstrate the improvement of the fitting with the fiducial model. The dashed line gives the *GLAST* integral sensitivity (1 yr  $5\sigma$ : McEnery et al. 2004). The dot-dashed and dotted lines correspond to the *HXMT* ( $10^5\text{s } 3\sigma$ : Li et al. 2006) and *NuSTAR* ( $10^6\text{s } 3\sigma$ : [www.astro.caltech.edu/~avishay/zwicky1/ppts/Harrison.ppt](http://www.astro.caltech.edu/~avishay/zwicky1/ppts/Harrison.ppt)) sensitivities, respectively.

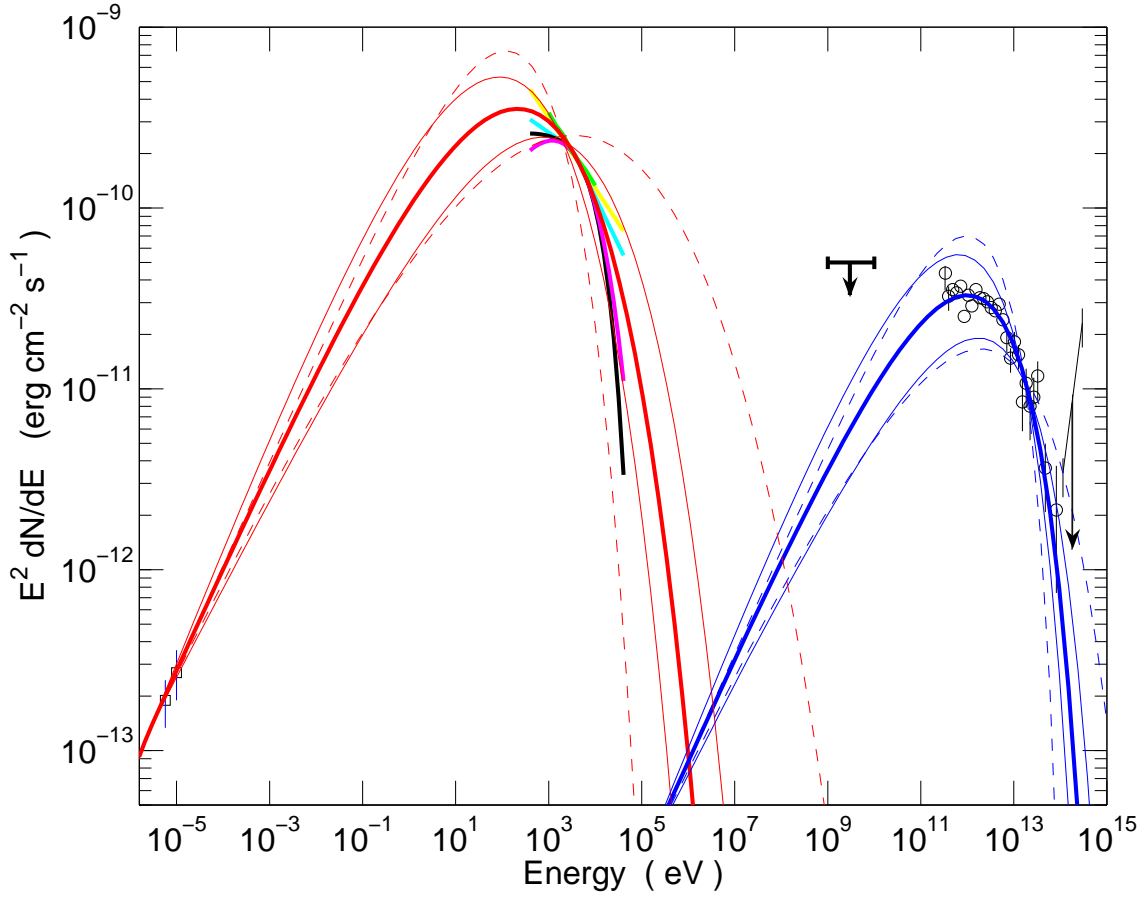


Fig. 2.— Dependence of the emission spectrum on  $\beta$  and  $p$ .  $B = 12$  G.  $\gamma_c$  and  $E_e$  are adjusted to fit the radio to X-ray fluxes. The two dashed lines are for  $p = 1.85$  and  $\beta = 0.25$  and 1.0. The thin solid lines are for  $\beta = 0.5$  and  $p = 1.7$  and 2.0.